JOINT EUROPEAN TORUS

JET–P(89)86

C.S. Pitcher, M. Bures, L. de Kock, S.K. Brents, N.A. Gottardi,
G.M. McCracken, M.F. Stamp, P.C. Stangeby, D.D.R. Summers
and J.A. Tagle

Some Effects of ICRH Heating on the JET Boundary Plasma

X Some Effects of ICRH Heating on the JET Boundary Plasma

C.S. Pitcher[1], M. Bures, L. de Kock, S.K. Brents[2], N.A. Gottardi, G.M. McCracken[2], M.F. Stamp, P.C. Stangeby[3], D.D.R. Summers and J.A. Tagle

JET-Joint Undertaking, Culham Science Centre, OX14 3DB, Abingdon, UK

[1]Canadian Fusion Fuels Technology Project, Toronto, Canada. Present address: Princeton Plasma Physics Laboratory, P.O. Box 451, Princeton, NJ 08543, USA
[2]Culham Laboratory UKAEA, Abingdon, Oxfordshire, United Kingdom
[3]Institute for Aerospace Studies University of Toronto and JET Joint Undertaking

Preprint of Paper to be submitted for publication in
Journal of Vacuum Science and Technology

ABSTRACT.

Detailed boundary plasma measurments are reported for a special series of ICRH discharges in JET in which Z_{eff} remained constant over a range of powers. This behaviour is examined using a relatively simple model of particle and energy balance using the measured parameters of the scrape-off layer. Carbon influx measurements from the limiter are compared with those calculated from the model.

1 Introduction

To attain thermo-nuclear conditions in JET large quantities of auxiliary heating will be required [1]. In the case of ion cyclotron resonance heating (ICRH) the addition of power to the plasma results in the release of both fuel and impurities from the internal surfaces of the vacuum vessel [2-12]. The release of impurities is undesirable since it reduces the thermo-nuclear yield of the discharge due to a reduction of the central fuel temperature and concentration. Uncontrolled release of fuel reduces the possibility of density control.

Impurities released during ICRH heating fall into two classes. First, those which originate from the Faraday screens, which in JET during the present campaign was composed of nickel. It has recently been shown that the rate of release of screen material is proportional to the applied power [13] with the resulting impurity content of the discharge rising to significant levels during repeated long pulse, high power discharges. In this campaign, however, with fewer high power discharges and with the screen being covered with a layer of carbon, the nickel contribution to the radiation and dilution is small.

The second source of impurities is the limiters and wall, which in JET during this experiment is primarily carbon. One speculation is that the ICRH produces energetic particles which subsequently hit the internal surfaces of the vessel and sputter carbon impurities [14-16]. Although such energetic particles have indeed been observed with probes [17], no consistent picture has yet emerged, in part because of the lack of detailed data. Another source of impurities results from the interaction of the thermal boundary plasma with the limiter surface subject to an increase in the power reaching the boundary [12,16,18-20]. It has been shown that this power is in part due to the direct coupling of ICRH power to the plasma boundary, with the remainder arriving at the boundary after diffusing from the plasma core [2-4].

Whether the release of impurities is due to a small energetic population and/or due to the thermal background, due to direct edge deposition of ICRH power or core deposition, it is clear that detailed boundary plasma data is needed before the primary cause of the impurity influx can be identified. Similar uncertainties exist as to the source of the additional fuel that is desorbed during the application of ICRH power.

In order to investigate the processes by which fuel and carbon impurities are released from the vessel surfaces, a specific sequence of discharges with varying ICRH power, for which the wall and limiter condition was well defined and constant, have been studied in JET with a

number of edge-specific diagnostics. The purpose of the present publication is to report these detailed measurements and to show that the observed behaviour can be partially explained using simple power and particle balance considerations. It should be noted that the results and interpretation presented in this paper are for a particular set of discharge conditions (whose main characteristic is that Z_{eff} remains constant over a range of heating powers), and different results and interpretations are obtained with different machine conditions.

2 Experiment

The JET vessel cross-section is shown in Fig. 1, illustrating the positions of the belt limiters and ICRH antennas. The belt limiter consists of two complete toroidal bands of graphite tiles positioned approximately 0.9 m above and below the mid-plane, whilst the ICRH antennas are located at 8 discrete toroidal locations and are similarly protected with graphite tiles [21].

The boundary plasma is diagnosed with a reciprocating Langmuir probe, two CCD cameras (vertical and tangential), limiter thermocouples and visible spectroscopy. The positions of the reciprocating probe and vertical CCD camera are shown in Fig. 1. The probe can penetrate from outside the plasma to several centimetres inside the last closed flux surface (LCFS) and return in a period of ~ 0.5 s, producing a complete radial profile of edge density n_e and electron temperature T_e. The vertical CCD camera has a carousel of interference filters, centered on intense spectral lines of C I, C II, C III, D_α and He I, which can be revolved between discharges. The tangential camera (not shown in Fig. 1) is equipped with a D_α filter and simultaneously views the two belt limiters and a single ICRH antenna through a tangential window. Both cameras are absolutely calibrated. In addition to the camera viewing, the upper belt limiter is monitored with a visible spectrometer with an optical multi-channel analyzer. To determine the radiated power from the discharge the plasma is viewed with horizontal and vertical bolometer arrays. The power deposited to the belt limiters and the ICRH protection structures can be determined using thermocouples embedded in the graphite tiles.

3 Results

These experiments refer to a set of discharges performed on one day when the wall was well-conditioned and reproducible performance was obtained. The discharges were all at a plasma current of 3.3 MA and a toroidal field of 3.4 T in deuterium with varying levels ICRH

heating at 32 MHz using He-3 minority species and monopole phasing resulting in a wave-number peaked at $k_{\|}$~0. The plasma position in these experiments is such that contact is primarily with the belt limiters, with a balance ratio of ~ 0.5. The balance ratio is defined to be the ratio of the spatially-integrated D_α signals at the upper belt to that at the lower, as determined by the tangential camera. The total interaction with the protection tiles of the RF antennas is small, as similarly determined using the spatially-integrated D_α signal, typically accounting for ~ 10% of the combined D_α signal from the two belt limiters. The plasma volume, plasma surface area, total limiter contact area and safety factor are $115m^3$, $150m^2$, ~$13m^2$ and $q_\psi = 5.0$, respectively. The belt limiter and wall are maintained at approximately constant temperature between discharges at values of 165 C and 300 C, respectively.

The central plasma parameters as functions of time during ~ 14 MW of ICRH are shown in Fig. 2. The heating pulses are nominally 4 s long, with a 2 s period during which the discharge reaches a steady state, ie giving essentially constant levels for the total input power P_{tot}, volume-averaged density $< n_e >$, radiated power P_{rad} and Z_{eff}. For comparison, results from an Ohmic discharge (Ω) are also given in Fig. 2. At the end of the heating pulse, at t ~ 13 s, the conditions in the ICRH discharge revert to the Ohmic values.

Although the vessel is well-conditioned in these experiments (well-conditioned in the sense that any effect associated with a previous vacuum opening is negligible, ie the oxygen content of the discharge is low, the density reaches a steady state value during the heating pulse and dilution and radiation are due primarily to carbon impurities), the application of ICRH power results in an increase of the particle content of the discharge, as indicated by $< n_e >$ in Fig. 2. This increase is reproducible within this sequence of discharges and depends mainly on the ICRH power. In other cases, depending on the run history of the machine, for example, whether helium discharges had been performed prior to the sequence, the amount and the rate of the density rise can be different resulting in a different overall behaviour [22]. These experiments were not immediately preceded by any such conditioning. The dependence of the volume-averaged density on power is shown in Fig. 3. Also shown is the edge electron density $n_e(a)$ as determined by the reciprocating probe. While the edge density appears to scale in a linear fashion with power, the particle content has a weaker dependence.

The dependences of a number of plasma conditions on ICRH power are given in Fig. 4 and discussed below:

$n_e(a), T_e(a)$ The density and temperature at the LCFS as determined by the reciprocating probe. While the density is approximately proportional to input power, the edge electron temperature rises less strongly. The data set is a subset of data presented in [22,23].

λ_Γ The particle flux e-folding distance in the scrape-off layer as determined by the reciprocating probe. This is constant at $\lambda_\Gamma \sim 2.1 cm$ at the position of the probe. Because of the compression of the magnetic flux surfaces the corresponding value at the mid-plane is ~ 1.2 cm [24]. The electron temperature e-folding distance λ_T is also determined by the probe; at low power, $\lambda_T \sim 2\lambda_\Gamma$, which increases with ICRH power to a value of $\lambda_T \sim 5\lambda_\Gamma$ at 14 MW. Because λ_Γ is short and λ_T relatively long we take T_e constant over the SOL for the purposes of this paper.

Γ_C, Γ_D The total influx of carbon and deuterium from the belt limiters determined by the cameras using the intensity of the C I and D_α lines and theoretical photon effiencies [25,26]. In the case of deuterium, it is assumed that the recycled particles leave the graphite surface as D_2 molecules and are broken down in the plasma by the following reaction route,

$$D_2 \rightarrow D_2^+ \rightarrow D + D^+$$

Thus, for each molecule recycled only one D atom is produced which then radiates according to its photon efficiency [26]. As with the edge density, Γ_C and Γ_D are approximately proportional to the input power. Similar data using the C II charge state was reported in [7].

P_{rad}/P_{tot} The radiated power fraction as determined by the bolometer arrays. This decreases slightly with power but is approximately constant at $P_{rad}/P_{tot} \sim 0.4$.

Z_{eff} The effective charge of the central discharge based on the visible bremsstrahlung is approximately constant at $Z_{eff} = 2.3$.

W_{LIM} The energy deposited in the belt limiters during the heating pulse based on the bulk temperature rise of the tiles using thermocouples. The temperature rise associated with the Ohmic part of the discharges is subtracted out and the values indicated result from the averaging of a number of thermocouples in the upper and lower belt limiter. W_{LIM} is approximately proportional to the input power. The balance ratio, based on the ratio of the energy deposited in the upper belt to that deposited in the lower belt, was ~ 0.5, similar to that found for the D_α signals.

For this series of discharges we summarize the results from Fig. 4: $n_e(a)$, Γ_C, Γ_D and W_{LIM} are approximately proportional to the input power whilst $T_e(a)$, λ_Γ, P_{rad}/P_{tot} and Z_{eff} vary only slightly.

The power conducted and convected to the limiter P_{con} as determined by three independent methods is shown in Fig. 5 as a function of the input power P_{tot}. In the first method, the radiated power as determined by the bolometer is simply subtracted from the input power with the result that throughout the power scan, P_{con}/P_{tot}~0.61. In the second method, the bulk temperature rise of the carbon tiles with their known thermal capacity is used giving P_{con}/P_{tot}~0.36, which is significantly smaller than the value determined by the bolometer. In the third method the power incident on the limiter is based on the probe measurements of $n_e(a)$, $T_e(a)$, λ_Γ and assuming $\gamma = 10$ [27], where γ is the energy deposited per ion-electron pair normalized by T_e. In this case a value of P_{con}/P_{tot}~0.23 is arrived at which is in reasonable agreement with the thermocouple measurements and is similarly in disagreement with the bolometer.

4 Discussion

The main result from this series of discharges is that Z_{eff} remains approximately constant over a large range of ICRH powers. The behaviour of the boundary plasma parameters are controlled to a large extent by a net release of fuel from the vessel surfaces by an unknown desorption process. The additional fuel results in the edge density $n_e(a)$ rising approximately in proportion to the applied power while the edge electron temperature $T_e(a)$ rises only slightly.

It will be shown in this discussion that the observed qualitative behaviour can be reasonably well explained using simple power and particle balance considerations. Considering the complicated nature of the SOL interaction with the limiter, it is not surprising that quantitative discrepancies exist between the following simple model and the observations. These can only be resolved by more extensive diagnostics and modelling that takes into account all of the complexities.

4.1 Power Balance

The power added to the discharge is either radiated or convected/conducted to the limiter,

$$P_{tot} = P_{rad} + P_{con} \qquad [1]$$

The radiated power is,

$$P_{rad} = \; < n_e >< n_C > LV \qquad [2]$$

where V is the plasma volume and L is the volume-averaged radiated power coefficient [28]. This becomes

$$P_{rad} = \; < n_e > \tau_C L \Gamma_C \qquad [3]$$

where we have used

$$< n_C > \equiv \frac{\tau_C \Gamma_C}{V} \qquad [4]$$

where τ_C is the carbon ion confinement time. In theory, L is a function of $n_e\tau_C$ and T_e [29]; however, in practice, the empirical observation in JET is that L is constant to within a factor ~ 2 [13]. This simplifies the treatment of the radiated power because in general in most tokamaks the product of density and particle confinement time $< n_e > \tau_p$ is also a constant [30] and thus Eq. 2 becomes

$$P_{rad} \sim R_C \Gamma_C \qquad [5]$$

where

$$R_C \equiv < n_e > \tau_C L \sim constant \qquad [6]$$

where R_C is effectively the energy radiated per carbon atom influx, which is approximately a constant.

To see that $< n_e > \tau_C$ is indeed a constant in this experiment, the product can be determined using the experimentally measured density $< n_e >$, Z_{eff} and carbon influx Γ_C. From the quasi-neutrality condition and the definition of Z_{eff} we obtain,

$$< n_e > \tau_C = \frac{(Z_{eff} - 1) < n_e >^2 V}{Z(Z-1) \quad \Gamma_C} \qquad [7]$$

where Z is the fully-stripped carbon ion charge, Z = 6. The experimentally derived values of $< n_e > \tau_C$ using Eq. 7 at different ICRH powers appear in Fig. 6. One can see that a constant value of $< n_e > \tau_C \sim 3x10^{18} sm^{-3}$ is obtained.

The power conducted/convected to the limiter is approximately [31],

$$P_{con} = \gamma(\Gamma_D + Z_B \Gamma_C) k T_e(a) \qquad [8]$$

where Z_B is the average charge of the carbon ions in the boundary plasma, typically ~ 4 [32]. We have assumed that within the SOL the electron temperature is radially constant. Using Eqs. 5 and 8 the power balance becomes

$$P_{tot} = R_C \Gamma_C + \gamma(\Gamma_D + Z_B \Gamma_C) k T_e(a) \qquad [9]$$

The increase in ICRH power P_{tot} must therefore manifest itself either as a change in the edge electron temperature or the particle fluxes incident on the limiter or some combination of both. Since the experimental observation is that the change in the electron temperature is relatively small, the increased power loss must result primarily from increased particle fluxes according to Eq. 9.

4.2 Impurity Production

The ratio of influxes Γ_C/Γ_D depends on the sputtering yields for deuterons Y_D and carbon ions Y_C at the graphite limiter [33],

$$\frac{\Gamma_C}{\Gamma_D} = \frac{Y_D}{1 - Y_C} \qquad [10]$$

This expression neglects sources of carbon other than the graphite limiters, ie assumes that the wall and Faraday screen sources of carbon are small. Since the sputtering yields depend on the respective ion energies and these in turn depend on the edge electron temperature, then the ratio of fluxes is a function of the edge electron temperature, eg

$$\frac{\Gamma_C}{\Gamma_D} = f(T_e) \qquad [11]$$

A constant value of T_e thus implies a constant ratio of carbon flux to deuterium flux, as approximately observed. From Fig. 4 the mean value of the edge electron temperature during the power scan is $T_e \sim 55eV$. Using this value to calculate the sputtering yields [34], the flux ratio is expected to be $\Gamma_C/\Gamma_D \sim 0.06$ (assuming T_e to be constant within the SOL), a factor of ~ 3 lower than observed, $\Gamma_C/\Gamma_D \sim 0.2$. The variation of Γ_C/Γ_D over the temperature range considered (42 - 65 eV) is about 20%. This calculation assumes a D^+ impact energy of $5T_e \sim 275eV$ giving a yield of $Y_D \sim 0.035$ and a carbon ion (assumed to be C^{+4} [32]) impact energy of $14T_e \sim 770eV$ giving a yield of $Y_C \sim 0.38$ [31]. The discrepancy between the observed and the calculated flux ratios may be due partly to the experimental error in converting spectral intensities to particle influxes; this is estimated to be a factor of ~ 2. However, the discrepancy might also be explained by an enhancement of the sputtering yields due to particles striking the limiter at angles other than normal incidence [7]. An enhancement of the above normal incidence yields by a factor of ~ 1.8 would give agreement between the expected and the observed effective yields according to Eq. 10.

4.3 Impurity Content, Z_{eff}, Dilution

The central concentrations of the carbon and deuterium are approximately related by the expression [35],

$$\frac{n_C(0)}{n_D(0)} = \frac{\Gamma_C \lambda_{iz}^C}{\Gamma_D \lambda_{iz}^D} \qquad [12]$$

where λ_{iz} is the effective penetration distance into the plasma of the respective particles from the limiter source. It appears from Monte Carlo simulations using the LIM impurity transport code and the NIMBUS neutral hydrogenic transport code [35,36] that under most conditions, $\lambda_{iz}^D/\lambda_{iz}^C \sim 2$ and thus, using the experimental flux ratio $\Gamma_C/\Gamma_D \sim 0.2$, the central carbon concentration is

predicted to be $n_C(0)/n_D(0)\sim0.1$, giving $n_D(0)/n_e(0)\sim0.6$ and $Z_{eff}\sim2.9$, compared with what is experimentally observed, $n_C(0)/n_D(0)\sim0.06$ and $n_D(0)/n_e(0)\sim0.74$, which are obtained from $Z_{eff}\sim2.3$. This is typical of the general finding that the central impurity concentration is less than predicted using Eq. 12, theoretical penetration distances and the experimentally deduced influxes. Nevertheless, Eq. 12 does predict a constant value for the central dilution (ie a constant Z_{eff}) given that Γ_C/Γ_D and $\lambda_{iz}^D/\lambda_{iz}^C$ are both approximately constant.

4.4 Power Losses

Figure 5 gives the power conducted/convected to the limiter P_{con} based on the radiated power from the bolometer, the limiter temperature rise and the Langmuir probe. The resulting values for the ratio P_{con}/P_{tot} are 0.61, 0.36 and 0.23, respectively. One possible explanation for the discrepancy between the bolometer and the other two measurements may lie in the fact that the radiation is highly assymetric within the plasma volume, being concentrated in the boundary plasma at large major radii, in the vicinity of the belt limiters [37]. The bolometer may not be able to properly determine the total radiation with localized radiation sources. This may also be the explanation as to why the limiter temperature rise is somewhat higher than predicted by the Langmuir probe, ie local radiation in the vicinity of the limiter is absorbed by the graphite tiles. An alternative explanation is that a small population of highly energetic ions in the boundary plasma is produced by the ICRH. Such ions could deposit significant power without registering on the Langmuir probes. From other studies [38] such unaccounted power is estimated to be no more than ~ 15% of the total input power and thus, while it might explain the difference between the thermocouples and the Langmuir probe, it cannot explain the larger difference between these two and the bolometer. A third possible explanation for the discrepancy between the thermocouples and the Langmuir probe is that secondary electron emission from the graphite limiter surface enhances the power deposition. This would effectively increase the value of γ above the value of 10 used in Fig. 5.

It is clear from the experiment that the radiated power fraction P_{rad}/P_{tot} is roughly independent of input power. However, the actual value varies by a factor of ~ 2 depending on which diagnostic is used - the bolometer, the thermocouples or the Langmuir probe. These gives values for P_{rad}/P_{tot} of ~ 0.39, ~ 0.64 and ~ 0.77, respectively. In the case of the bolometer we can obtain the value of R_C, the energy radiated per carbon atom influx, from the slope of P_{rad} plotted against

the carbon influx Γ_C, Fig. 7. This is ~ 11 keV/particle and from similar graphs using the thermocouples and the Langmuir probe then values of ~ 18 keV/particle and ~ 21 keV/particle are obtained. These are all signficantly higher than predicted from theory under these conditions, ie we would expect R_C values in the range of 3 to 7 keV/particle [29]. The corresponding values of the radiated power coefficent L, determined using Eq. 6 and the experimentally derived value of $< n_e > \tau_C \sim 3x10^{18} sm^{-3}$, are $L \sim 5.8x10^{-34} Wm^3$, $\sim 9.5x10^{-34} Wm^3$ and $\sim 1.1x10^{-33} Wm^3$, which are all in reasonable agreement with the earlier empirical observation in JET [13].

4.5 Central Density

The application of the ICRH heating causes an increase in the limiter fluxes proportional to the additional heating power. The edge fuelling increases the edge density and consequently increases the total particle content. At constant edge electron temperature and with constant cross-field particle transport (although not conclusive, the constant value of λ_Γ, Fig. 4, indicates that the cross-field diffusion coefficient in the boundary remains approximately constant) we expect in steady state that $n_e(a) \propto \Gamma_D \propto < n_e >^2$ [36]. This behaviour is shown in Fig. 8, where Γ_D, derived from the spectroscopic intensities at the belt limiters, has been plotted against the square of the volume-averaged electron density, ie $< n_e >^2$. Although a linear relationship is clearly demonstrated in Fig. 8, it is also clear that the straight line does not pass through the origin as expected, ie the relationship appears to breakdown at low densities. It may be that at low densities the limiter particle source is no longer dominant and recycling at the wall needs to be included. Such behaviour has indeed been shown in Monte Carlo neutral simulations [39].

It should be noted that the observed increase of the flux of deuterium entering the plasma consists of two components [2-4]: one with a short rise-time (< 10 ms) which reacts to the direct absorption of a fraction of the ICRH power in the plasma boundary and one with a longer time constant corresponding to power diffusing to the scrape-off layer after absorption in the plasma core. Under steady state conditions the observed deuterium fluxes from the limiter reflect the overall rise in the plasma deuterium inventory rather than a direct observation of the original desorption process since fuel recycling is the dominant process. The deuterium release related to the application of ICRH power is one of the main factors controlling the behaviour of the edge parameters (the other is the increase in the power conducted to the edge). The amount of desorption and the balance between the fast and slow source depends on the machine condition. In this particular series of discharges the total desorption raises the deuterium content in such a way that

the edge electron temperature rises only slightly with corresponding consequences for the carbon sputtering and Z_{eff}. Under other limiter and wall conditions the rise in edge electron temperature with power can be more pronounced.

5 Conclusion

The application of ICRH power in JET with carbon limiters produces an increase in the plasma deuterium inventory due to an unknown desorption process. The increase in plasma density results in an increase in the deuterium and carbon influxes from the limiter and a reduction in the thermo-nuclear yield of the discharge. Taking the experimentally observed edge plasma parameters and using sputtering data from the literature the behaviour of Z_{eff} and related parameters as a function of power can be understood. The nearly constant edge temperature observed in these discharges maintains a constant sputtering yield at the limiter and thus a constant Z_{eff} over the experimental range of ICRH powers. The calculated effective sputtering yield is a factor of 3 below the directly observed one. This might be explained by experimental uncertainties in the interpretation of the spectroscopic data or by angle of incidence effects. Another discrepancy is the central impurity concentration which is generally observed to be smaller by a factor of ~ 2 than predicted by theoretical penetration distances and the observed influx. A third discrepancy is that the radiated power is significantly higher by a factor of 2 to 4, depending on which diagnostic is used to infer P_{rad}, than expected for a given influx or concentration of carbon in the plasma. The power conducted to the limiters obtained from bolometric measurements is higher than that calculated from edge plasma parameters or from limiter temperature measurements. The last two agree within experimental errors. The discrepancy might be explained by unobserved asymmetries in all measurements.

While the behaviour of the boundary plasma properties during ICRH are qualititatively understood (quantitatively to within a factor of 2 to 4), it still remains to explain the desorption process which results in the boundary fluxes. This has not been considered in the present study, but a model addressing the desorption process is discussed in another publication [40].

References

(1) R J Bickerton and the JET-Team, Plasma Phys Contr Fusion 29 (1987) 1219.

(2) M Bures, V P Bhatnagar, M P Evrard, A Gondhalekar, J Jacquinot, T T C Jones, P D Morgan and D F H Start, Proceedings of the 14th European Conference on Controlled Fusion and Plasma Physics, Madrid, June 1987, 11D II, 722.

(3) M Bures, V P Bhatnagar, J Jacquinot, P Morgan and D F H Start, Plasma Phys Contr Fusion 30 (1988) 1833.

(4) S K Erents, J A Tagle, G M McCracken, H W Brinkschulte, S J Fielding, T Huld, P C Stangeby and L de Kock, J Nucl Mat 145-147 (1987) 231.

(5) M F Stamp, K H Behringer, M J Forrest, P D Morgan and H P Summers, J Nucl Mat 145-147 (1987) 236.

(6) M F Stamp, K H Behringer, M J Forrest, P D Morgan and H P Summers, J Nucl Mat 162-164 (1989) 404.

(7) M F Stamp, M J Forrest, P D Morgan and H P Summers, Proceedings of the 16th European Conference on Controlled Fusion and Plasma Physics, Venice, March 1989, 13B IV, 1513.

(8) U Samm, H L Bay, P Bogen et al, Plasma Phys Contr Fusion 29 (1987) 1321.

(9) U Samm, P Bogen, H Hartwig, J Nucl Mat 162-164 (1989) 24.

(10) B Schweer, H L Bay, W Bieger et al, Proceedings of the 13th European Conference on Controlled Fusion and Plasma Physics, Schliersee, 1986, I 399.

(11) J-M Noterdaeme, G Janeschitz, K McCormick et al, Proceedings of the 14th European Conference on Controlled Fusion and Plasma Physics, Madrid, June 1987, 11D II, 678.

(12) A S Wan, B Lipschultz, F S McDermott and J L Terry, J Nucl Mat 162-164 (1989) 292.

(13) K Behringer et al, 11th IAEA Conf Plas Phys Controlled Fusion Research (Kyoto, Japan), IAEA CN 47/A-IV-1 (1986).

(14) J Tachon, in "Physics of Plasma-Wall Interactions in Controlled Fusion", Eds. D E Post and R Behrisch, NATO ASI Series, Plenum Press, New York (1986) 1005.

(15) D Manos, T Bennett, R Budny, S Cohen, S Kilpatrick and J Timberlake, J Vac Sci Technol A2 (1984) 1348.

(16) S A Cohen, S Bernabei, R Budny et al, J Nucl Mat 128/129 (1984) 280.

(17) D M Manos, P C Stangeby, R V Budny, S A Cohen, S Kilpatrick and T Satake, J Nucl Mat 129 (1984) 319.

(18) A Grosman and TFTR Group, J Nucl Mat 128/129 (1984) 292.

(19) H L Manning, J L Terry, B Lipschultz et al, Nucl Fusion 26 (1986) 1665.

(20) K Odajima, H Matsumoto, H Kimura et al, Proc Int Symp Heating in Toroidal Plasmas, Rome 1984, I 243.

(21) P E Stott and the JET Team, J Nucl Mat 162-164 (1989) 3.

(22) J A Tagle, S K Erents, M Bures et al, J Nucl Mat 162-164 (1989) 282.

(23) S K Erents, P J Harbour, S Clement et al, Proceedings of the 16th European Conference on Controlled Fusion and Plasma Physics, Venice, March 1989, 13B III, 939.

(24) P C Stangeby, J A Tagle, S K Erents and C Lowry, Plas Phys and Contr Fusion 30 (1988) 1787.

(25) I I Sobelman, L A Vainshtein and E A Yukov, "Excitation of Atoms and Broadening of Spectral Lines", Springer-Verlag, Berlin, 1981.

(26) L C Johnson and E Hinnov, J Quant Spectro Radiat Transfer 13 (1973) 333.

(27) P C Stangeby, in "Physics of Plasma-Wall Interactions in Controlled Fusion", Eds. D E Post and R Behrisch, NATO ASI Series, Plenum Press, New York (1986) 41.

(28) S K Erents, J A Tagle, G M McCracken, P C Stangeby and L C J M de Kock, Nucl Fusion 28 (1988) 1209.

(29) P G Carolan and V A Piotrowicz, Plas Phys 25 (1983) 1065.

(30) P C Stangeby, J Nucl Mat 145-147 (1987) 105.

(31) P C Stangeby, J Phys D 20 (1987) 1472.

(32) G F Matthews, J Nucl Mat 162-164 (1989) 38.

(33) G M McCracken and P C Stangeby, Plas Phys Controlled Fusion 27 (1985) 1411.

(34) J Bohdansky, in "Data Compendium for Plasma-Surface Interactions", Nucl Fusion Special Issue 1984, 61.

(35) P C Stangeby, C Farrel, S Hoskins and L Wood, Nucl Fusion 28 (1988) 1945.

(36) R Simonini, J Spence and P C Stangeby, submitted for publication and Contrib Plas Phys 28 (1988) 459.

(37) N Gottardi, Joint European Torus (1989), private communication.

(38) J Jacquinot, Joint European Torus (1989), private communication.

(39) D N Ruzic, D B Heifetz and S A Cohen, J Nucl Mat 145-147 (1987) 527.

(40) C S Pitcher, Fusion Engineering and Design, to be published.

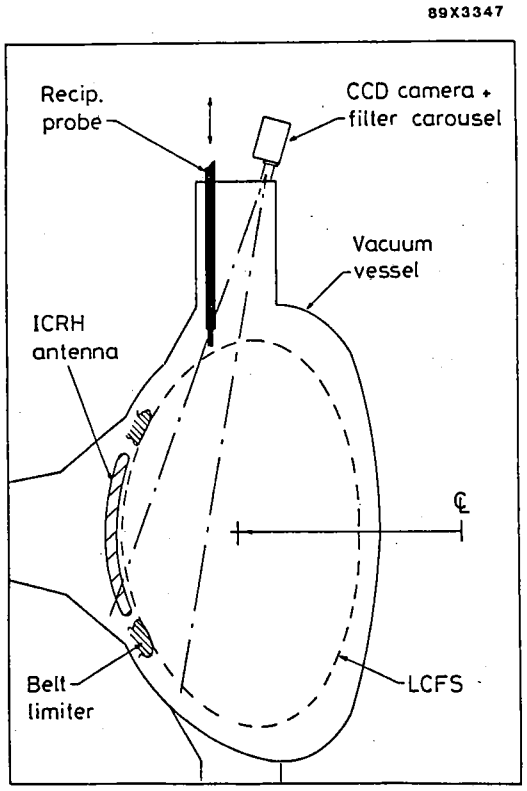

Fig. 1 A cross-section of the JETvacuum vessel showing the positions of the discrete ICRH antennas, the toroidal belt limiters, the reciprocating Langmuir probe and the vertical CCD camera.

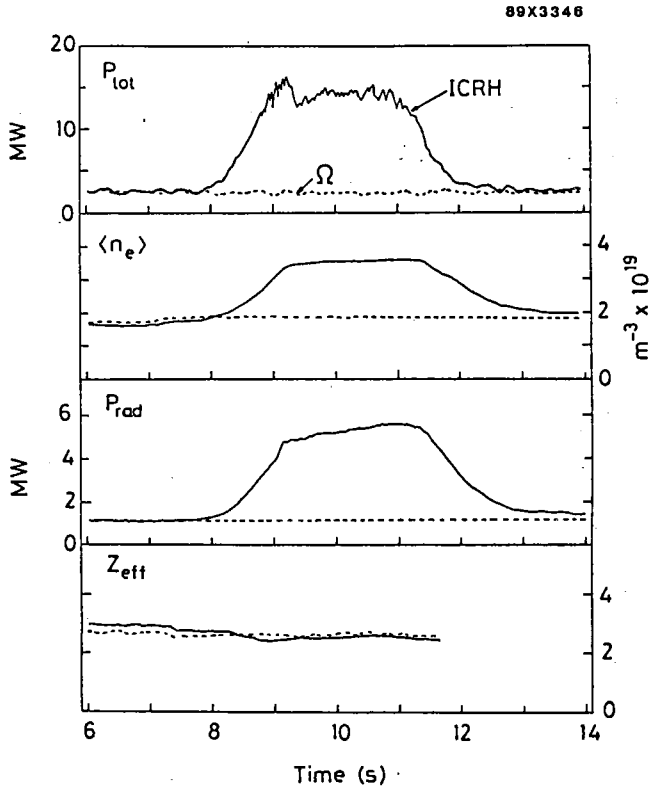

Fig. 2 The time behaviour of the central discharge parameters during a 14MW ICRH heated discharge and an Ohmicly heated discharge (Ω): the total input power P_{tot}, the volume-average density $<n_e>$, the radiated power as determined by the bolometer arrays P_{rad} and the effective charge of the discharge Z_{eff} as determined by visible bremsstrahlung.

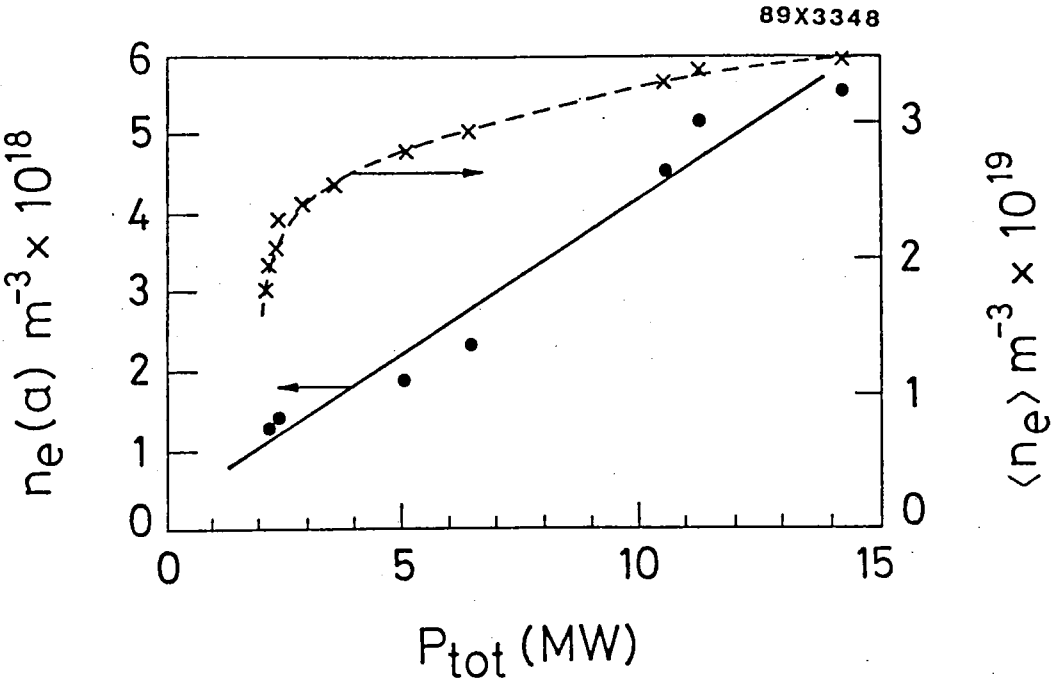

Fig. 3 The steady-state volume-averaged density $< n_e >$ and edge density n_e (a) as functions of total input power P_{tot}.

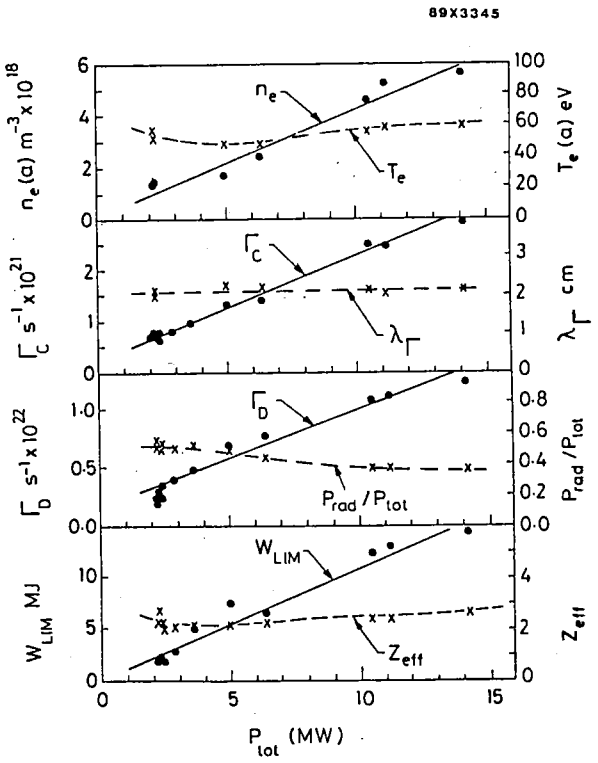

Fig. 4 Various discharge parameters during the steady state portion of the heating pulse as functions of the total input power P_{tot}: the edge density n_e (a), electron temperature T_e (a) and particle flux e-folding distance $\lambda\Gamma$ as determined with the Langmuir probe, the influxes of carbon Γ_C and deuterium Γ_D from the belt limiters as determined from spectral emissions, the radiated power fraction P_{rad}/P_{tot} from the bolometer arrays, the energy deposited in the belt limiters W_{LIM} from thermocouple measurements and Z_{eff} from visible bremsstrahlung.

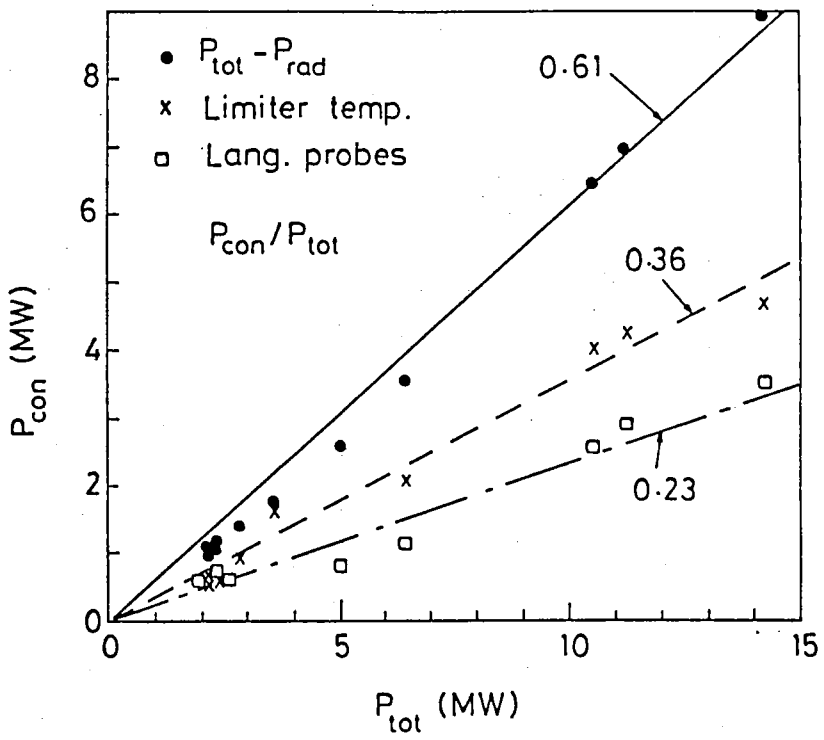

Fig. 5 The power conducted/convected to the limiter P_{con} as a function of the total input power P_{tot} as determined by (A) subtracting the radiated power obtained with the bolometer arrays from the total input ($P_{tot} - P_{rad}$) (B) the bulk temperature rise of the limiter graphite tiles with their known thermal capacity (C) the Langmuir probe measurements of n_e (a), T_e (a), $\lambda\Gamma$ and assuming $\gamma = 10$ [27], where γ is the energy deposited per ion-electron pair normalized by T_e ($\lambda\Gamma$ is assumed to be infinite).

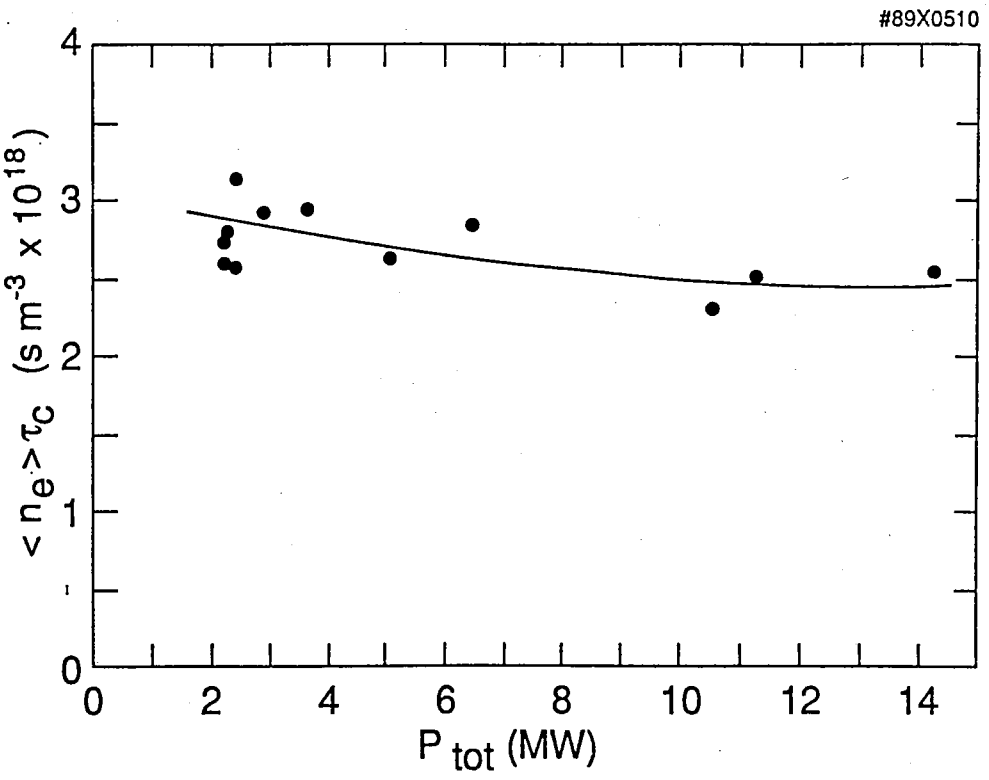

Fig. 6 The product $< n_e > \tau_C$, as determined from experimental data using Eq.7, as a function of total input power P_{tot}.

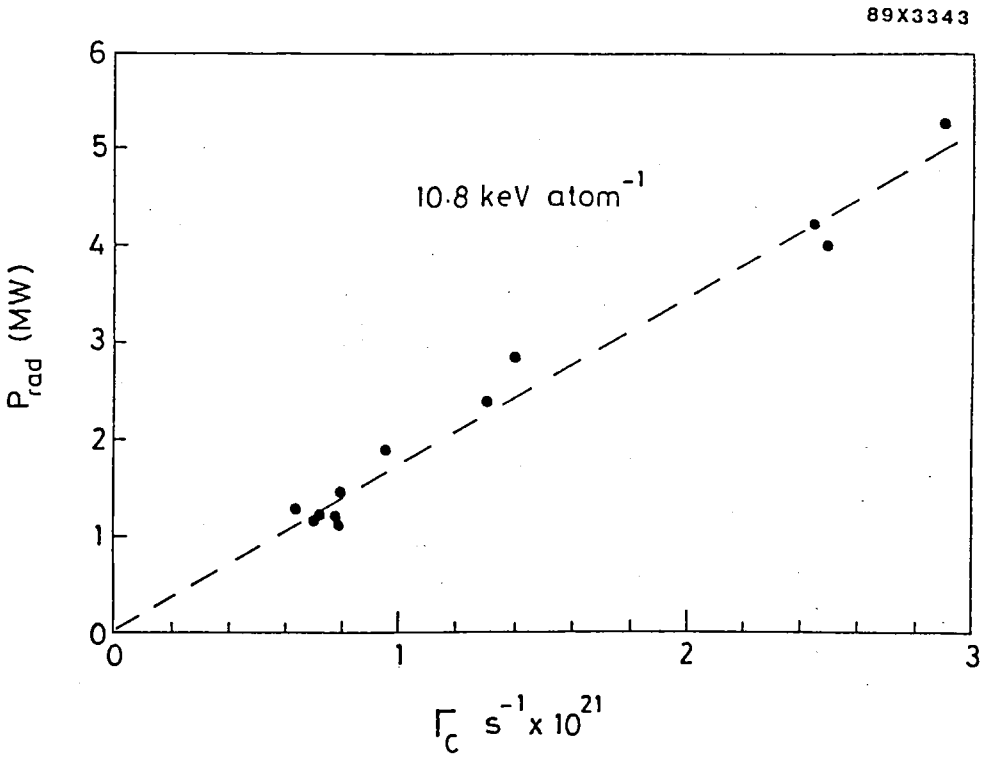

Fig. 7 The radiated power P_{rad} from the bolometer arrays plotted as a function of the carbon influx from the belt limiters Γ_C. The slope of the line is $R_C = 10.8$ keV/atom, the energy radiated per carbon atom influx.

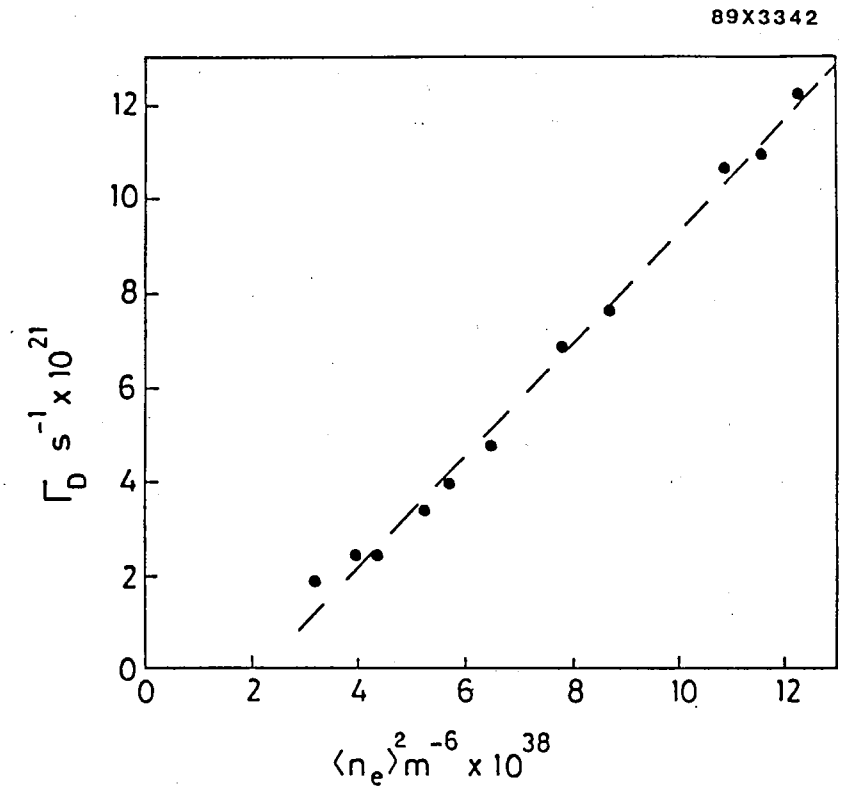

Fig. 8 The deuterium influx from the belt limiters Γ_D plotted against the volume-averaged density squared $<n_e>^2$.